

Supporting Information

Tailoring the mechanical properties of polymer nanocomposites via interfacial engineering

Naishen Gao¹, Guanyi Hou¹, Jun Liu^{1,2,3,4*}, Jianxiang Shen⁵, Yangyang Gao¹, Alexey V. Lyulin^{6*}

and Liqun Zhang^{1,2,3,4,7}

¹Key Laboratory of Beijing City on Preparation and Processing of Novel Polymer Materials, Beijing University of Chemical Technology, People's Republic of China

²Beijing Engineering Research Center of Advanced Elastomers, Beijing University of Chemical Technology, People's Republic of China

³Engineering Research Center of Elastomer Materials on Energy Conservation and Resources, Beijing University of Chemical Technology, People's Republic of China

⁴Beijing Advanced Innovation Center for Soft Matter Science and Engineering, Beijing University of Chemical Technology, 100029 Beijing, People's Republic of China

⁵ College of Materials and Textile Engineering, Jiaying University, Jiaying 314001, People's Republic of China

⁶Theory of Polymers and Soft Matter and Center for Computational Energy Research, Department of Applied Physics Technische Universiteit Eindhoven, 5600 MB Eindhoven, The Netherlands

⁷State Key Laboratory of Organic-Inorganic Composites, Beijing University of Chemical Technology, 100029 Beijing, People's Republic of China

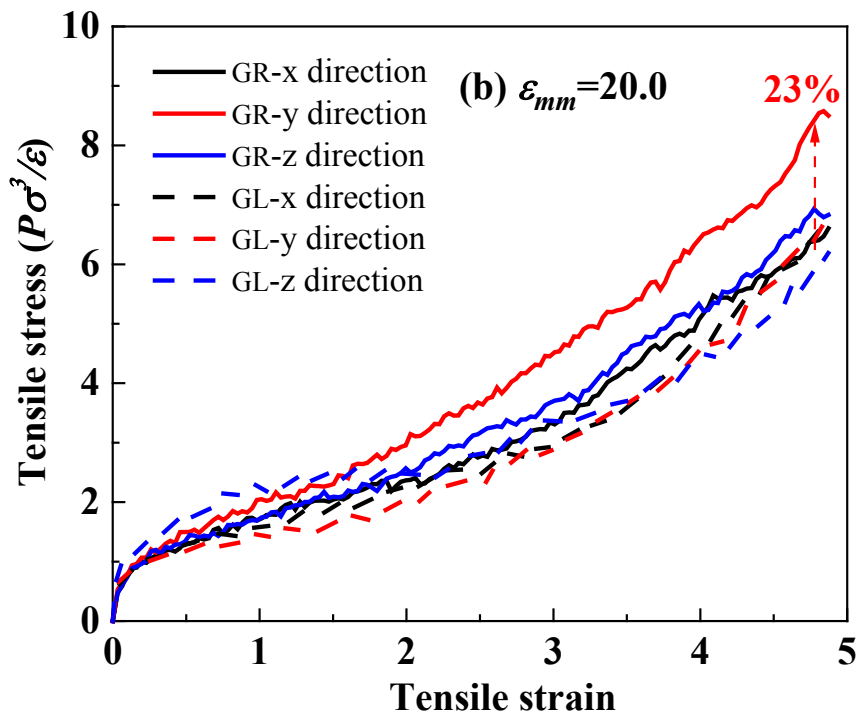
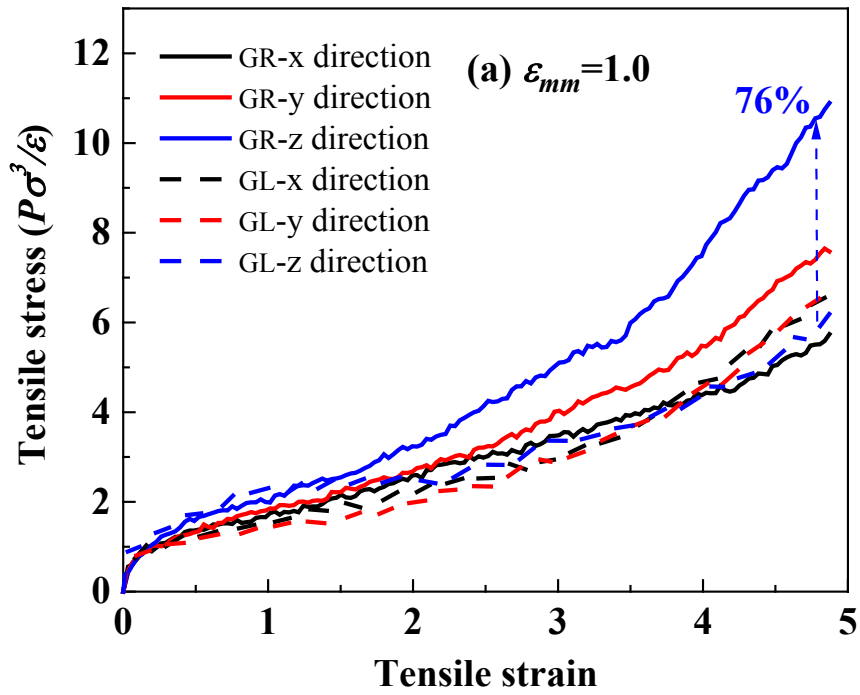
S1. The effect of flexible matrix chains

The matrix chains are set as flexible chains ($k = 0.0$). To allow the matrix chains threading through the rings better, the repulsion between the matrix chains is increased by changing ε_{mm} from 1.0 to 20.0, during the first equilibration step. After

*Corresponding author: liujun@mail.buct.edu.cn or a.v.lyulin@tue.nl.

the second equilibration step, taking two extreme cases ($\varepsilon_{mm} = 1.0$ and 20.0) as examples, the stress-strain curves during the uniaxial deformation are shown in Fig. S1(a) and Fig. S1(b). The amount of stress increase has been calculated in GR system relative to GL system in the corresponding direction (calculated by the stress at the maximum strain). It can be clearly seen that the stress increase only by $\sim 70\%$ in the Z direction for $\varepsilon_{mm} = 1.0$ and by $\sim 20\%$ in the Y direction for $\varepsilon_{mm} = 20.0$, indicating that the increasing of ε_{mm} during the first equilibration step does not improve the mechanical properties effectively.

By analyzing the snapshots in Fig.S1(c), we find that the flexible matrix chains will aggregate in the interior region of the grafted rings. The ideal interlocked structure is not formed, and the matrix chains are too flexible to thread through the grafted rings effectively. So, enhancing the stiffness of the matrix chains is necessary.



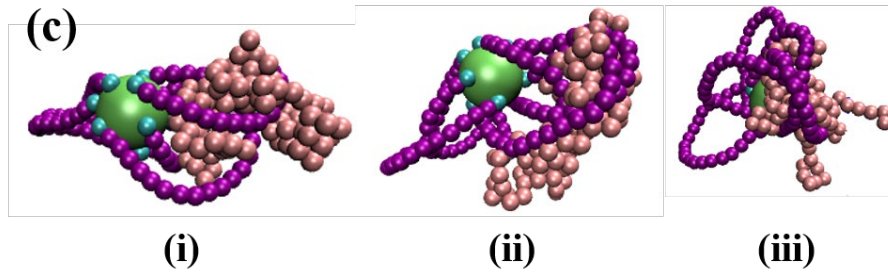


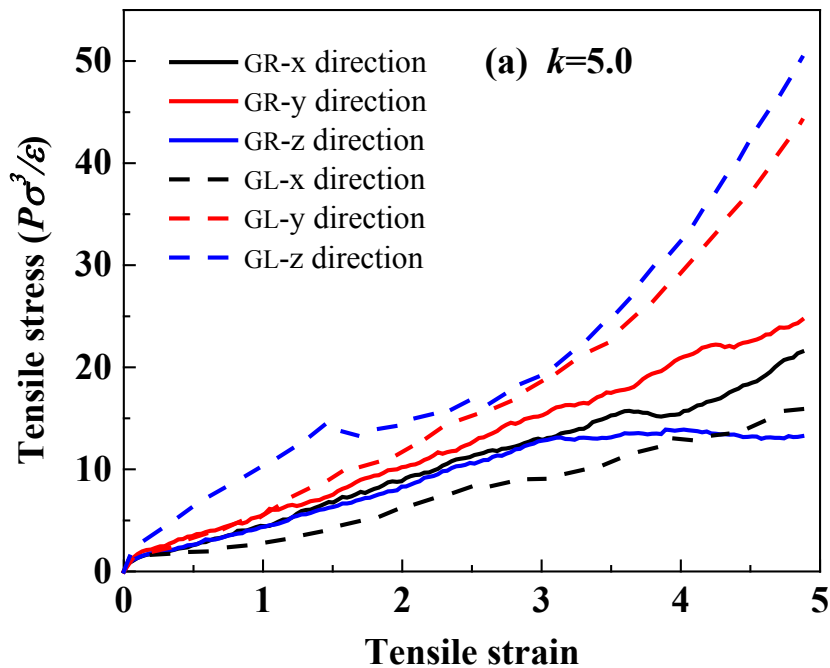
Fig.S1 The stress-strain behavior of the grafted-ring (GR) system and the grafted-linear (GL) system in three deformation directions: (a) $\varepsilon_{mm}=1.0$, (b) $\varepsilon_{mm}=20.0$. Black, red and blue colors represent X , Y and Z direction, respectively. (c) The snapshots of NP (green beads), grafted rings (purple spheres) and matrix chains (pink spheres) around the rings, cyan spheres represent the head atoms of the grafted chains bonded to NP surface, $\varepsilon_{mm}=1.0$.

S2. The effect of stiff matrix chains

The composite consisting of the stiff matrix chains has been investigated next with the same grafted chains as before. The stiffness of matrix chains has been varied by changing the parameter k in Eq.4, from $k = 5.0$ to $k = 30.0$. Taking two extreme cases ($k = 5.0$ and $k = 30.0$) as examples, the stress-strain behavior has been investigated, the results are shown in Fig. S2. We observe that, when $k = 5.0$, the stress at the maximum strain of GL system is much higher than that of GR system except the X direction. The GR system not only has no effect on stress enhancement, but also is worse than the GL system. We think the reason is that the grafted rings portion bear much less uniaxial deformation than the linear structure, since its two ends are fixed on the NP surface in the GR system.

As the stiffness of the matrix chains increases, the grafted chains play a trivial role gradually in the stretching process, and the matrix chains occupy the dominant position. When $k = 30.0$, the Y -direction stress curve of GR system approaches the deformation curve in the X -direction of GL system; at the same time, these two curves

are much higher than other curves. Due to the large stiffness and mutual attraction of the matrix chains, they can self-assemble easily into a rod-like conformation. This is similar to the results of Shen *et al.*^{1,2} where they used the stiff nanorods containing several connected beads, leading to the anisotropy of the tensile stress. The best mechanical properties were acquired when the system was stretched along the direction parallel to the rods. As the direction of the maximum stress in the simulated composite is not known, the maximum stress can occur, for example, in the *Y*-direction for the GR system, and in the *X*-direction for the GL system. From the results above, it is not feasible to form a mechanically interlocked structure by increasing the stiffness of the matrix chains. The reason for that is when the matrix chains thread through the rings easily, they are also easy to be pulled out during the uniaxial deformation.



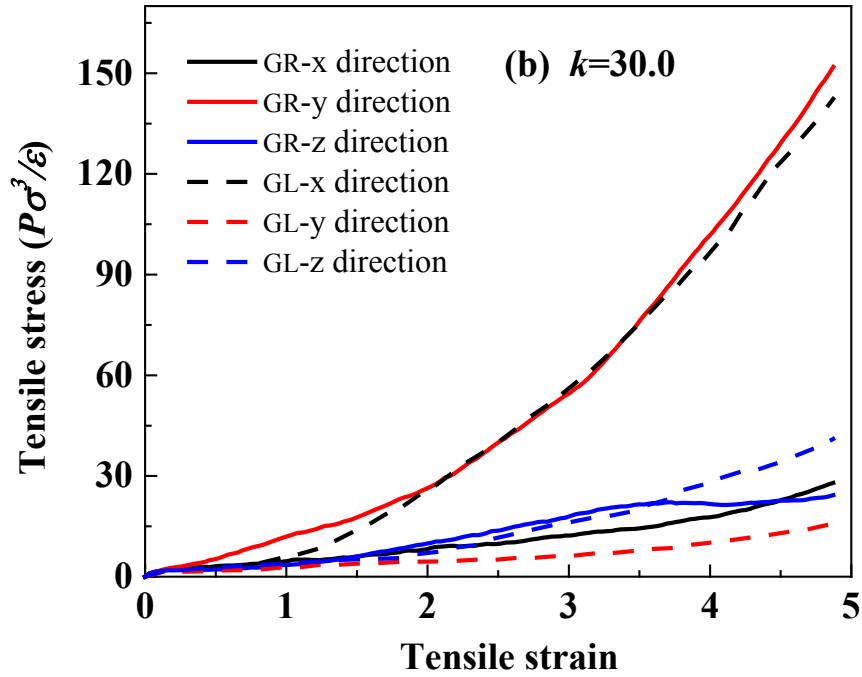


Fig.S2 The stress-strain behavior of the grafted-ring (GR) system and the grafted-linear (GL) system in three deformation directions with the matrix chains of different stiffness: (a) $k=5.0$, (b) $k=30.0$. Black, red and blue colors represent X, Y and Z direction, respectively.

S3. The structure of grafted rings with different angle θ_0

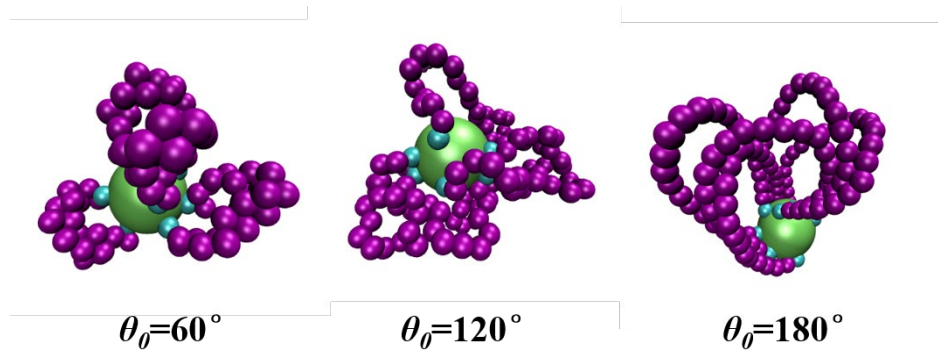
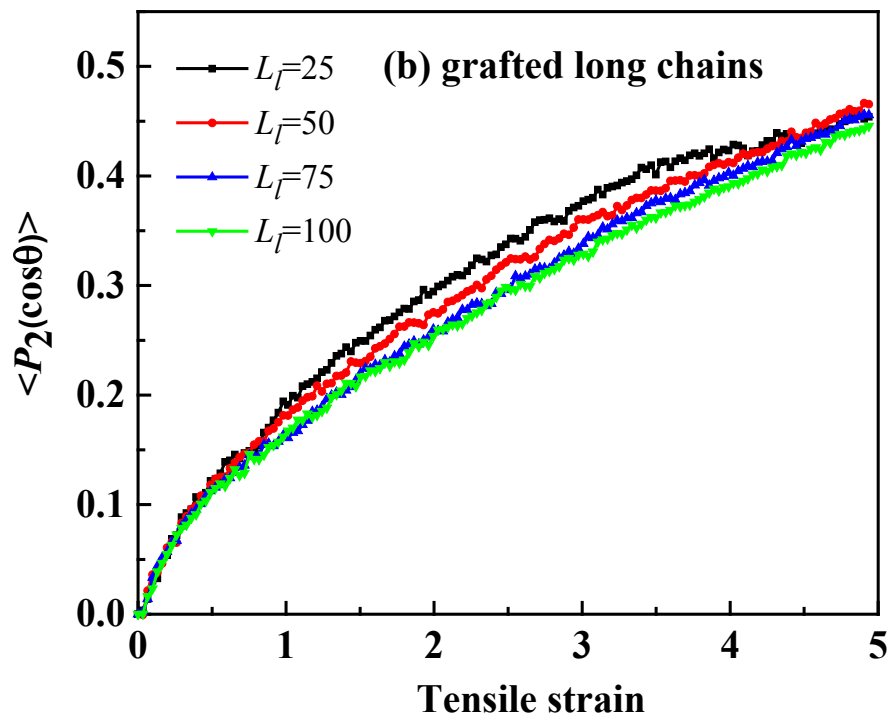
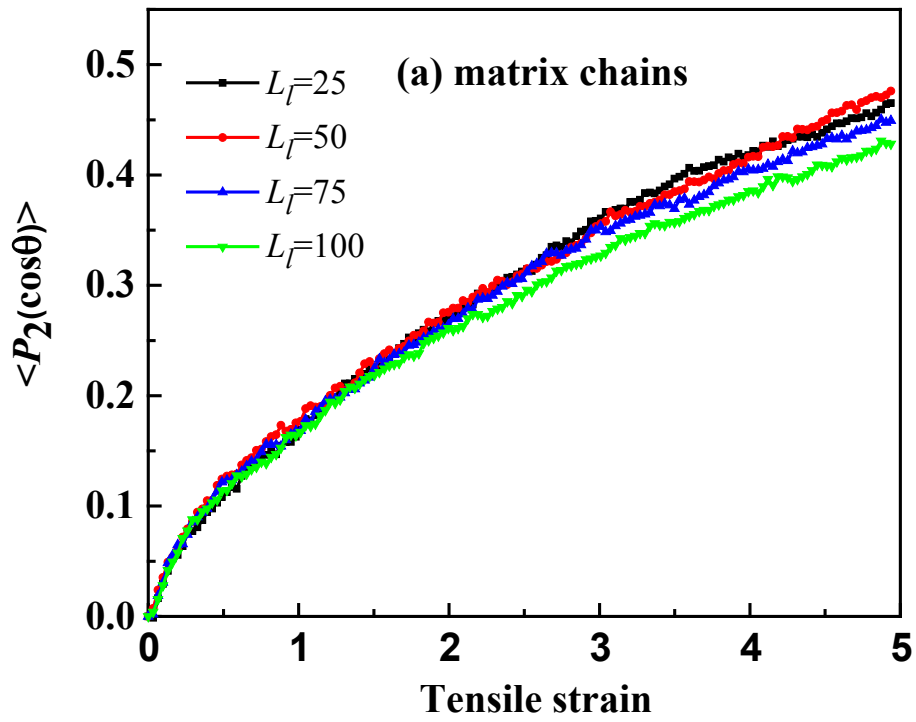


Fig.S3. Snapshots of NP and its grafted rings with different bending angle θ_0 .

S4. Bond orientation at $C_g=0.6$ during the deformation process



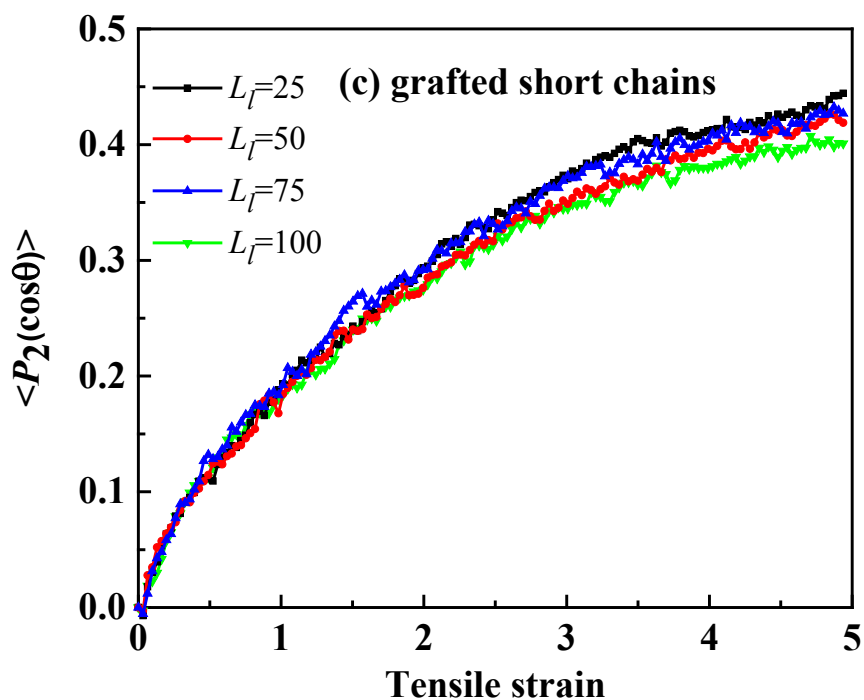
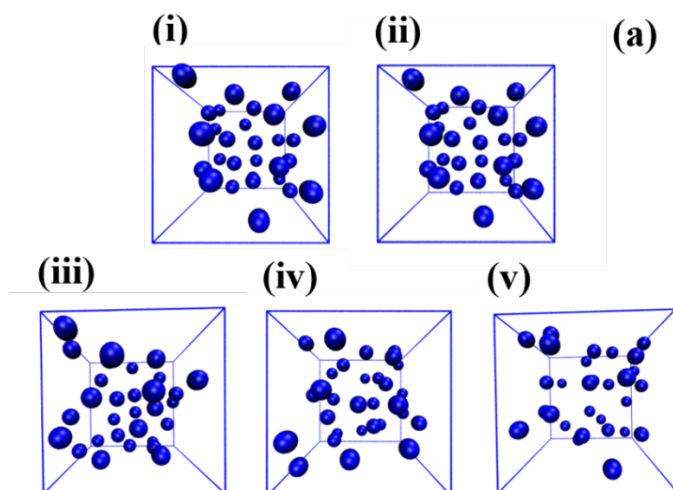


Fig.S4 The bond orientation of the matrix chains (a), the grafted long chains (b) and the grafted short chains (c) of the different systems during the deformation process.

S5. The dispersion of NPs at fixed graft density

The snapshots and the RDF between NPs are shown in Figs. S5(a) and S5(b). Clearly, with the increase of L_f , the NPs tend to separate, as evidenced by the systematic peak shifting to the right, and the absence of any maxima at $r = 4\sigma$.



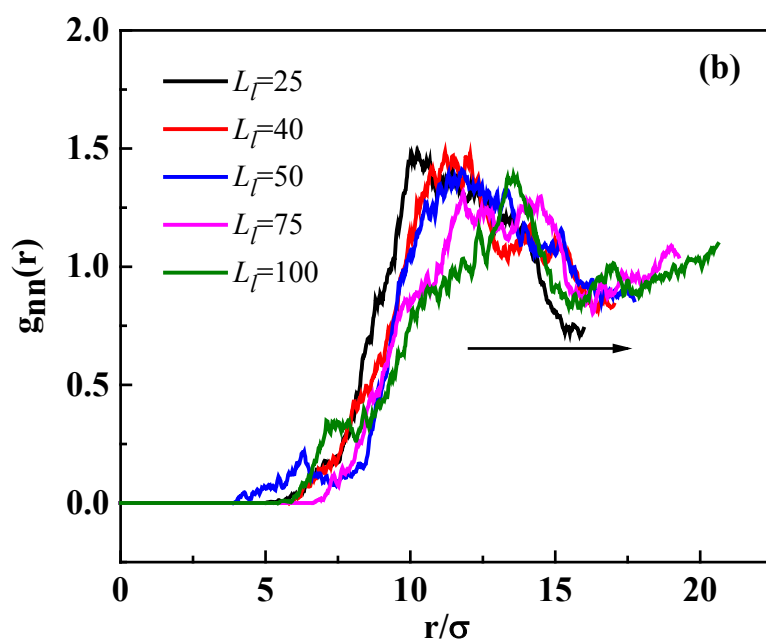


Fig.S5 (a) The snapshots of NPs corresponding to the different grafted long chains length L_l with increasing C_g : (i) $L_l=25$, (ii) $L_l=40$, (iii) $L_l=50$, (iv) $L_l=75$ and (v) $L_l=100$. The blue spheres denote NP cores. For clarity the polymer chains are not shown. (b) The radial distribution function of NP-NP with different L_l .

S6. The brush configuration -- radial distribution function of NP-grafted long chains, NP-grafted short chains and NP-matrix chains under different L_l .

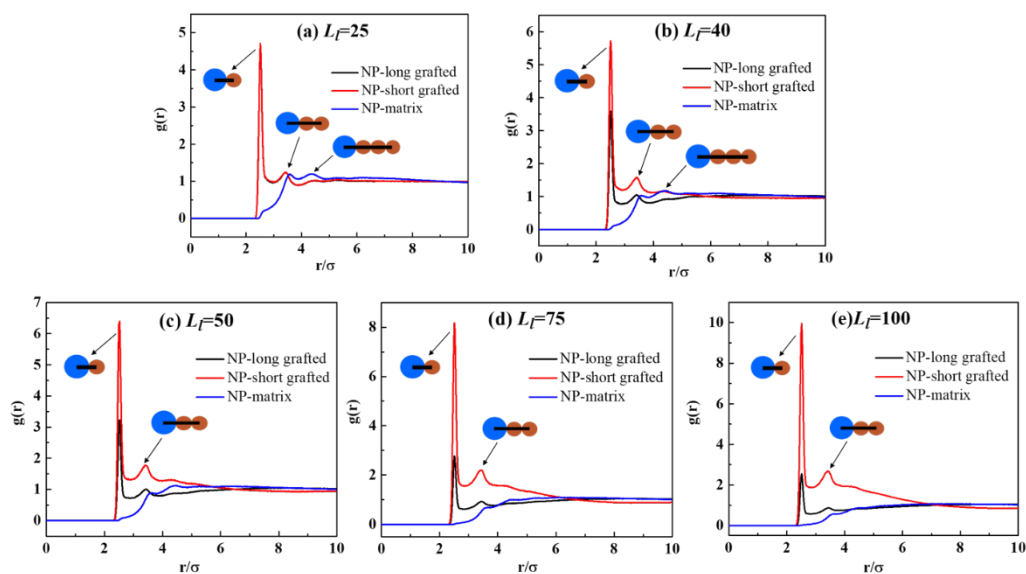


Fig.S6. The radial distribution functions (RDF) of NP-grafted long chains (black), NP-grafted short chains (red) and NP-matrix chains (blue) under different L_l .

Fig. S6 presents the radial distribution functions between the NPs center of mass and the grafted and matrix chains at different L_g . With the increase of L_g , the value of the first peak increases for short grafted chains. The opposite tendency is seen for the long grafted chains. This indicates that the longer L_g , the easier the grafted short chains are distributed within the first layer outside the NPs spherical shell; the grafted long chains are further away from the NPs. The common consensus is that the dense grafted chains can act as shielding layers which protect the NPs from aggregation. At the same time, the dense grafted short chain layer can effectively elongate the sparsely grafted long chains, and then promote the penetration of the grafted chains into the matrix chains, the so-called “elongation effect”. The peak values of the NP-matrix chain RDF decrease gradually. This shows that the excluded volume effect of the grafted chains increases upon increasing L_g . The matrix chains do not easily enter the interior of the brush, and are distributed in the periphery. These phenomena are attributed to the increase of the non-bonded interactions between the matrix chains and the grafted long chains with increase of L_g , while the non-bonded interactions between the matrix chains and the grafted short chains decrease, as shown in Fig.8(c).

S7. Bond orientation of the matrix chains during the deformation process

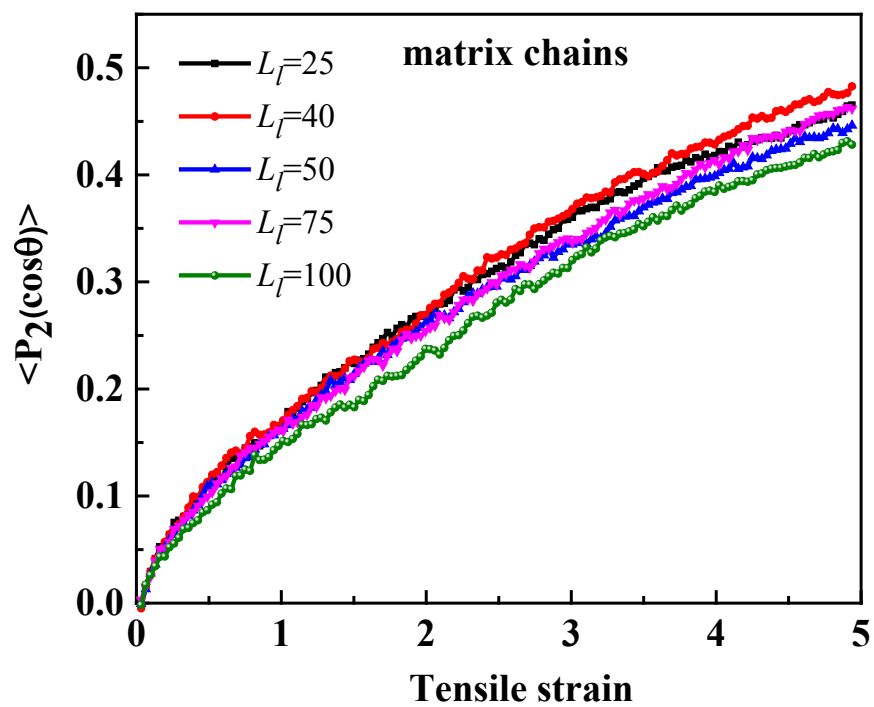


Fig.S7 The effect of the grafted long chains length L_l on the bond orientation of the matrix chains.

REFERENCES

1. J. Shen, X. Li, X. Shen and J. Liu, *Macromolecules*, 2017, **50**, 687-699.
2. J. Shen, X. Li, L. Zhang, X. Lin, H. Li, X. Shen, V. Ganesan and J. Liu, *Macromolecules*, 2018, **51**, 2641-2652.